EVALUATION OF FAST NEUTRON FLUENCE FOR KORI UNIT 3 PRESSURE VESSEL

CHOON SUNG YOO*, BYOUNG CHUL KIM, KEE OK CHANG, SAM LAI LEE and JONG-HO PARK[1]
Korea Atomic Energy Research Institute
150 Deokjin-dong, Yuseung-gu, Daejeon 305-353, Korea
[1]Chungnam National University
220 Gung-dong, Yuseung-gu, Daejeon 305-764, Korea
*Corresponding author. E-mail : csyoo@kaeri.re.kr

Received April 10, 2006
Accepted for Publication July 3, 2006

Three-dimensional neutron flux and fluence of Kori Unit 3 were evaluated using the synthesis technique described in Regulatory Guide 1.190 for all reactor geometry. For this purpose DORT neutron transport calculations from Cycle 1 to Cycle 15 were performed using BUGLE-96 cross-section library. The calculated flux and fluence were validated by comparing the calculated reaction rates to the measurement data from the dosimetry sensor set of the 5th surveillance capsule withdrawn at the end of cycle 15 of Kori Unit 3. And then the best estimation of the neutron exposures for the reactor vessel beltline region was performed using the least square evaluation. These results can be used in the assessment of the state of embrittlement of Kori Unit 3 pressure vessel.

KEYWORDS : Surveillance, Embrittlement, Fluence, Vessel, Exposure

1. INTRODUCTION

In the assessment of the state of embrittlement of light water reactor (LWR) pressure vessels, an accurate evaluation of the neutron exposure of the beltline region of the vessel is required. In Appendix G to 10 CFR 50 [1], the beltline region is defined as "*the region of the reactor vessel shell material (including welds, heat affected zones and plates or forgings) that directly surrounds the effective height of the reactor core and adjacent regions of the reactor vessel that are predicted to experience sufficient neutron radiation damage to be considered in the selection of the most limiting material with regard to radiation damage*". Therefore, plant specific exposure assessments must include evaluations as a function of axial and azimuthal location over the entire beltline region.

Regulatory Guide 1.190, "Calculational and Dosimetry Methods for Determining Pressure Vessel Neutron Fluence" [2] describes state-of-the-art calculation and measurement procedures that are acceptable to the NRC staff for determining pressure vessel fluence. Also included in Regulatory Guide 1.190 is a discussion of the steps required to qualify and validate the methodology used to determine the neutron exposure of the pressure vessel wall. One important step in the validation process is the comparison of plant specific neutron calculations with available measurements.

This paper describes a neutron fluence assessment performed for Kori Unit 3 pressure vessel beltline region based on the guidance specified in Regulatory Guide 1.190. In this assessment, fast neutron exposures expressed in terms of fast neutron fluence (E > 1.0 MeV) were established for the beltline region of the pressure vessel. The exposure experienced by the reactor pressure vessel was determined on a fuel cycle specific basis for the first fifteen operating cycles (approximately 15.4 Effective Full Power Years (EFPY)).

Kori Unit 3 has an extensive plant specific measurement database from dosimetry included in the in-vessel capsules irradiated as an integral part of the Reactor Vessel Materials Surveillance Program [3]. To date, five in-vessel capsules have been withdrawn from the reactor at the end of Cycles 1, 4, 8, 12 and 15.

Using dosimetry evaluation methodologies that follow the guidance of Regulatory Guide 1.190, the neutron dosimetry sensor set from the 5th in-vessel surveillance capsule withdrawn at the end of Kori Unit 3 Cycle 15 was analyzed. These dosimetry evaluations were then used to validate the calculational models that were applied in the plant specific neutron transport analyses.

In this paper, the methodologies used to perform neutron transport calculations and dosimetry evaluations are described, the results of the plant specific transport calculations

are given for the beltline region of Kori Unit 3 pressure vessel and the comparisons of calculations and measurements are discussed.

2. METHODS

The exposure of Kori Unit 3 pressure vessel was developed on the basis of a series of cycle specific neutron transport calculations validated by comparison with plant specific measurements. Measurement data were obtained from in-vessel capsule irradiations. In this section, the neutron transport methodology and the dosimetry evaluation methodology are discussed.

2.1 Synthesized Neutron Flux

In performing the fast neutron exposure evaluations, plant specific forward transport calculations were carried out using the three-dimensional flux synthesis technique described in Section 1.3.4 of Regulatory Guide 1.190. The following synthesis approach was employed for all fuel cycles:

$$\phi(r,\theta,z,E) = \phi(r,\theta,E)\cdot\frac{\phi(r,z,E)}{\phi(r,E)}. \qquad (1)$$

Where $\phi(r, \theta, z, E)$ is the synthesized three-dimensional neutron flux distribution, $\phi(r, \theta, E)$ is the transport solution in R-θ geometry, $\phi(r, z, E)$ is the two-dimensional solution for a cylindrical reactor model using the actual axial core power distribution, and $\phi(r, E)$ is the one-dimensional solution for a cylindrical reactor model using the same source per unit height as that used in the R-θ two-dimensional calculation.

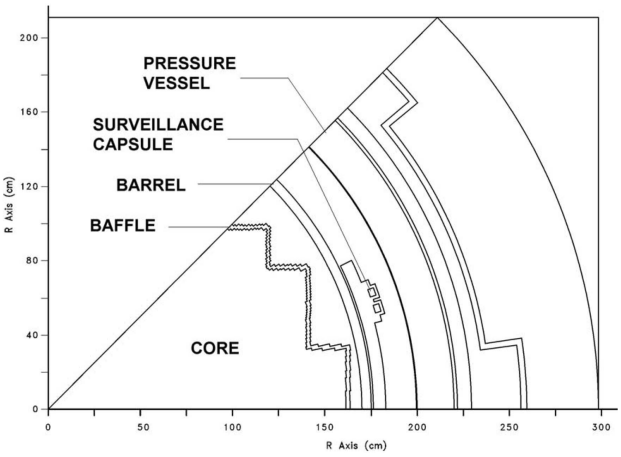

Fig. 1. Kori Unit 3 R-θ Geometry for Neutron Transport Calculations

All of the transport calculations were carried out using the DORT two-dimensional discrete ordinates code Version 3.1 [4] and the BUGLE-96 cross-section library [5]. The BUGLE-96 library provides a 67 group coupled neutron-gamma ray cross-section data set produced specifically for LWR application. In these analyses, anisotropic scattering was treated with a P_5 legendre expansion and the angular discretization was modeled with an S_{16} order of angular quadrature.

Figure 1 shows a plan view of the R-θ model of Kori Unit 3 reactor geometry at the core midplane. A single octant is depicted showing the arrangement of neutron pads and surveillance capsule attachments. In addition to the core, reactor internals, pressure vessel and primary biological shield, the models developed for these octant geometries also included explicit representations of the surveillance capsules, the pressure vessel cladding, the pressure vessel reflective insulation, and the reactor cavity liner plate.

From a neutronic standpoint, the inclusion of the surveillance capsules and associated support structure in the analytical model is significant. Since the presence of the capsules and structure has a marked impact on the magnitude of the neutron flux as well as on the relative neutron and gamma ray spectra at dosimetry locations within the capsules, a meaningful evaluation of the radiation environment internal to the capsules can be made only when these perturbation effects are properly accounted for in the analysis.

In developing the R-θ analytical models of the reactor geometry shown in Figure 1, nominal design dimensions were employed for the various structural components. Water temperatures and, hence, coolant density in the reactor core and downcomer regions of the reactor were taken to be representative of full power operating conditions (2775 MW). The reactor core was treated as a homogeneous mixture of fuel, cladding, water, and miscellaneous core structures such as fuel assembly grids, guide tubes, etc.

Figure 2 shows a sectional view of the R-Z model of Kori Unit 3 reactor. The model extends radially from the centerline of the reactor core out to a location inside the primary biological shield and over a fourteen foot axial span from an elevation one foot below to one foot above the active fuel region. The axial extent of the model was chosen to permit the determination of the maximum exposure of vessel materials in the beltline region opposite the reactor core.

As in the case of the R-θ models, nominal design dimensions and full power coolant densities were employed in the calculations. In this case, the homogenous core region was treated as an equivalent cylinder with a volume equal to that of the active core zone. The stainless steel former plates located between the core baffle and core barrel regions were also explicitly included in the model.

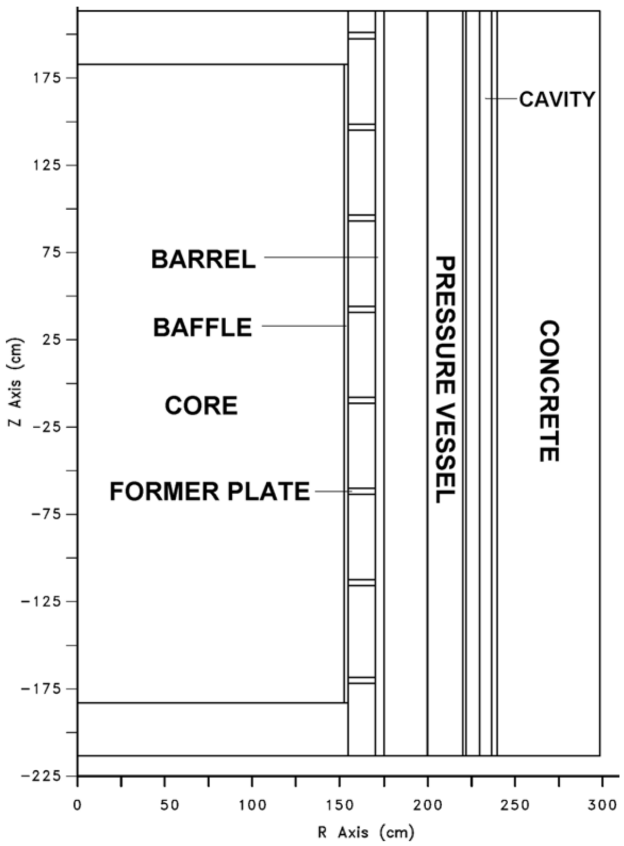

Fig. 2. Kori Unit 3 R-Z Geometry for Neutron Transport Calculations

The one-dimensional radial model used in the synthesis procedure consisted of the same radial mesh intervals included in the R-Z model. Thus, radial synthesis factors, $\phi(r, z, E) / \phi(r, E)$, could be determined on a meshwise basis throughout the entire geometry.

The SORCERY [6] computer code was used to prepare a fixed distributed source for DORT transport calculations. This code prepares a fixed distributed source in DORT X-Y, R-θ, or R-Z discrete ordinates transport theory code space mesh. Given initial U-235 enrichments and assembly burnup data, SORCERY properly accounts for the fission of U-235, U-238, Pu-239, Pu-240, Pu-241 and Pu-242.

The radial core burnup distributions were taken from the appropriate Nuclear Design Reports for the first fifteen operating cycles. For example, Figure 3 shows the radial burnup distributions for Cycle 9. And other important nuclear design data such as fuel assembly specific initial enrichments, and core average axial power distributions were also obtained from the respective design reports.

2.2 Synthesized Neutron Fluence

In Regulatory Guide 1.99, Revision 2 [7], the adjusted reference temperature (ART) for each material in the beltline region is given by the following expression:

$$ART = Initial\ RT_{NDT} + \Delta RT_{NDT} + Margin\ . \quad (2)$$

Where *Initial* RT_{NDT} is the reference temperature for the unirradiated material as defined in paragraph NB-2331 of Section III of the ASME Boiler and Pressure Vessel Code. ΔRT_{NDT} is the mean value of the adjustment in reference temperature caused by irradiation and should be calculated as follows:

$$\Delta RT_{NDT} = CF \cdot f^{(0.28-0.10\log f)}, \quad (3)$$

where CF(°F) is the chemistry factor, a function of copper and nickel content, and f (10^{19} n/cm^2, E > 1.0 MeV) is the fast neutron fluence evaluated for the irradiated vessel material. Therefore in the assessment of the state of embrittlement of pressure vessels, an accurate evaluation of the neutron fluence of the beltline region of the vessel is required.

Using the synthesized neutron flux of section 2.1, three-dimensional fast neutron fluence of equation (3) can be calculated as follows:

$$f(r,\theta,z) = \int\int_{1MeV}^{\infty} \phi(r,\theta,z,E,t)dEdt\ . \quad (4)$$

In equation (4) the time integration is performed from the initial startup of the reactor to the end of the irradiation. We define the cycle average three-dimensional neutron flux, which is representative of each cycle at full power, and we can calculate this value by using DORT with the cycle average radial power distribution. Let $\phi_i(r, \theta, z, E)$ be the cycle average neutron flux for the ith cycle. Then equation (4) can also be written as

$$f(r,\theta,z) = \sum_{i=1}^{n} [\int_{1MeV}^{\infty} \phi_i(r,\theta,z,E)dE]\Delta t_i\ , \quad (5)$$

where Δt_i is the full power operation time (sec) for the ith cycle and n is the last cycle of irradiation. $\phi_i(r, \theta, z, E)$ of the above equation can be obtained from equation (1) and Δt_i can be obtained from the reactor operation history database for each fuel cycle from the site.

2.3 Dosimetry Evaluations

Each operating reactor has a reactor vessel surveillance program that consists of six to eight surveillance capsules

H	G	F	E	D	C	B	A	
30161 46601 0.964	0 21295 1.249	17508 36926 1.139	17621 38007 1.195	0 22595 1.325	0 21957 1.287	11319 28153 0.987	29679 36008 0.371	8
0 21295 1.249	17598 36692 1.120	16969 36669 1.155	0 22914 1.344	19476 39039 1.147	14308 33761 1.141	0 17273 1.013	24467 30103 0.330	9
17508 36926 1.139	16925 36564 1.152	18825 38616 1.160	0 22663 1.329	19457 38688 1.128	0 19005 1.114	19546 30141 0.621		10
17621 38007 1.195	0 22859 1.340	0 22669 1.329	18568 38744 1.183	0 21407 1.255	0 17852 1.047	29846 35770 0.347		11
0 22595 1.325	19464 39021 1.147	19408 38666 1.129	0 21431 1.257	0 19224 1.127	28027 35940 0.464			12
0 21957 1.287	14258 33726 1.141	0 19018 1.115	0 17863 1.047	28338 36217 0.462				13
11319 28153 0.987	0 17270 1.013	19513 30116 0.622	29870 35794 0.347		BOC Assembly Burnup EOC Assembly Burnup Cycle Average Relative Power			14
29679 36008 0.371	24400 30026 0.330							15

Fig. 3. Radial Burnup Distributions and Cycle Average Relative Power for Kori Unit 3 Cycle 9

located between the core and the reactor vessel in the downcomer region near the reactor vessel wall. The neutron dosimetry sensors contained in these capsules provide a measurement at this location. Table 1 shows the reaction of interest by neutrons for each dosimetry sensor used in Kori Unit 3 surveillance program [8-15]. The use of dosimetry sensors such as those included in LWR surveillance programs does not yield a direct measure of the energy dependent neutron flux at the measurement location. Rather, the activation or fission process is a measure of the integrated effect that the time and energy dependent neutron flux has on the target material over the course of the irradiation period. An accurate assessment of the average flux and, hence, the integrated exposure (fluence) experienced by the sensors may be developed from the measurements only if the sensor characteristics and the parameters of the irradiation are well known. In particular, the following variables are of interest:

- The measured specific activity of each sensor
- The physical characteristics of each sensor
- The energy response of each sensor
- The operating history of the reactor
- The neutron energy spectrum at the measurement location

Following irradiation, the specific activity of each of the irradiated radiometric sensors is determined using the latest version of ASTM counting procedures [8-14] for each reaction. Following sample preparation and weighing, the specific activity of each sensor is determined using a high resolution gamma spectrometer. In the case of the multiple sensor sets, these analyses are performed by direct counting of each of the individual sensors, or, as is sometimes the case with U-238 and Np-237 fission monitors from in-vessel irradiations, by direct counting preceded by dissolution and

Table 1. Neutron Dosimetry Sensors Used in Kori Unit 3 Surveillance Program

Sensor Material	Reaction of Interest	Target Atom Fraction	90% Response Range(MeV)	Product Half-Life	Fission Yield(%)
Copper	$^{63}Cu(n,\alpha)^{60}Co$	0.6917	4.9 – 11.8	5.271 yr	
Iron	$^{54}Fe(n,p)^{54}Mn$	0.0585	2.1 – 8.3	312.1 dy	
Nickel	$^{58}Ni(n,p)^{58}Co$	0.6808	1.5 – 8.1	70.82 dy	
Uranium	$^{238}U(n,f)^{137}Cs$	0.9996	1.2 – 6.7	30.07 yr	6.02
Neptunium	$^{237}Np(n,f)^{137}Cs$	1.0000	0.4 – 3.5	30.07 yr	6.17
Cobalt-Al	$^{59}Co(n,\gamma)^{60}Co$	0.0015	thermal	5.271 yr	

chemical separation of cesium from the sensor.

The irradiation history of the reactor over its operating lifetime can be determined from the site operation history documents. Generally the operating data are obtained on a monthly basis from reactor startup to the end of the dosimetry evaluation period. For the sensor sets utilized in in-vessel monitoring, the half-lives of the product isotopes are long enough that a monthly histogram describing reactor operation has proven to be an adequate representation for use in radioactive decay corrections for the reactions of interest in the exposure evaluations.

FCALC [16] is an utility computer code which is used to analyze the data obtained from dosimetry sensors contained in surveillance capsules or other neutron irradiation geometries. Given, as input data, the reactor power history, nuclear data for the reactions of interest, and measured specific activities, FCALC calculates decay corrected saturated activities and reaction rates for a variable irradiation.

Having the measured specific activities, the operating history of the reactor, and the physical characteristics of the sensors, reaction rates referenced to full power operation are determined by FCALC from the following equation:

$$R = \frac{A}{N_0 F Y \sum_{j=1}^{n} \frac{P_j}{P_{ref}} C_j [1-e^{-\lambda t_j}][e^{-\lambda t_d}]}, \quad (6)$$

where,

- R = reaction rate averaged over the irradiation period and referenced to operation at a core power level of P_{ref} (rps/nucleus),
- A = measured specific activity (dps/gm),
- N_0 = number of target element atoms per gram of sensor,
- F = weight fraction of the target isotope in the sensor material,
- Y = number of product atoms produced per reaction,
- P_j = average core power level during irradiation period j (MW),
- P_{ref} = maximum or reference core power level of the reactor (2775MW for Kori Unit 3),
- C_j = calculated ratio of ϕ (E > 1.0Mev) during irradiation period j to the time weighted average ϕ (E > 1.0Mev) over the entire irradiation period,
- λ = decay constant of the product isotope (1/sec),
- t_j = length of irradiation period j (sec),
- t_d = decay time following irradiation period j (sec).

And the summation is carried out over the total number of monthly intervals comprising the irradiation period. The ratio (P_j / P_{ref}) accounts for month-by-month variation of power level within any given fuel cycle as well as multiple fuel cycles. Figure 4 shows the ratios, which were taken from the site history document. The ratio C_j can be calculated for each fuel cycle using the synthesized neutron flux (section 2.1) at the location of sensor set. A total 15 C_j ratios were obtained. For each sensor the reaction rate averaged over the irradiation period can be obtained by using each measured specific activity. In order to account for U-235 content, Pu-239 build-in in the U-238 sensor, and photo fission in the U-238 and Np-237 sensors, the reaction rate obtained from FCALC was corrected by using the correction methods described in Reference 17.

2.4 Validation of the Synthesis Neutron Flux

The synthesized neutron flux derived in section 2.1 at the measurement location can be validated by comparison the dosimetry sensor reaction rates between calculation and measurement. The measured reaction rates can be obtained using the methodology described in section 2.3 and the calculated reaction rates with uncertainty can be obtained by the following equation [18]:

$$R_i \pm \delta_{R_i} = \sum_g (\sigma_{ig} \pm \delta_{\sigma_{ig}})(\phi_g \pm \delta_{\phi_g}), \quad (7)$$

where R_i is the reaction rate of dosimeter i, ϕ_g is the neutron spectrum calculated at the location of dosimeter set, σ_{ig} is

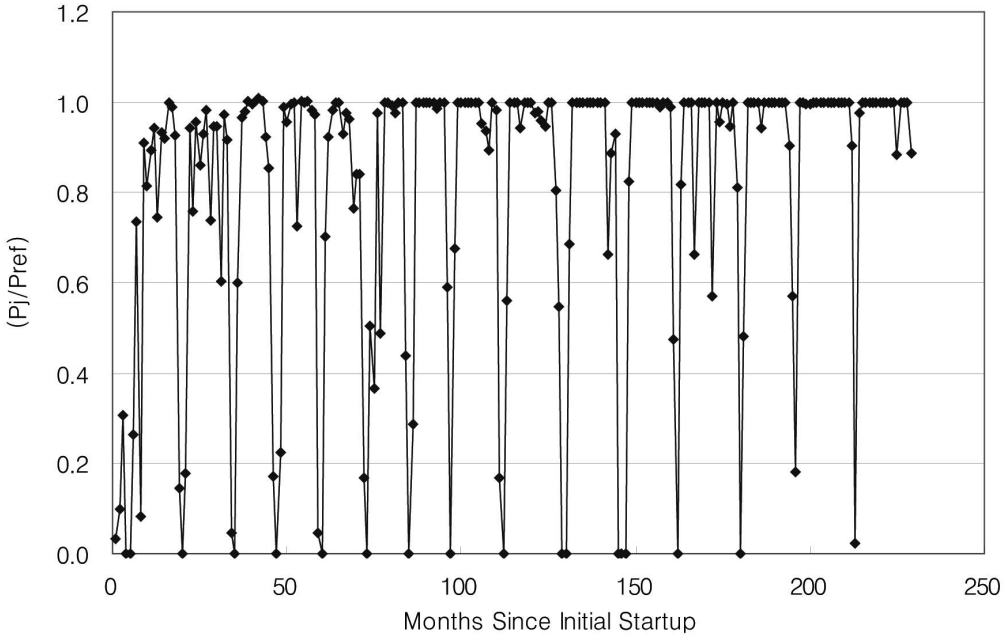

Fig. 4. Monthly Core Power History Since Initial Startup of Kori Unit 3

an appropriate multi-group dosimeter reaction cross-section, and δ_i is the associated uncertainty of parameter i. SAND/FERRET/INTVAL computer code sequence [19] is a good tool which can be used for this purpose. This code sequence produces calculated dosimeter reaction rates corresponding to the input neutron spectrum using dosimeter reaction cross-section such as SNLRML [20]. By comparisons of the calculated reaction rate to the measured reaction rate for each dosimeter, the calculated neutron flux can be validated.

And then the best estimate neutron flux can be also determined by combining the calculation and measurement results. The SAND/FERRET/INTVAL computer code sequence is also used to determine the best estimate neutron flux and the uncertainty at the measurement location from a least square fit. These results are combined with the reactor vessel fluence calculations to produce best estimate reactor vessel neutron fluence. Key inputs to the code package include measured reaction rates of each dosimeter and calculated trial spectrum at the measurement location. The dosimeter cross-sections are derived from the SNLRML dosimetry library [20].

SAND prepares a 53-group neutron spectrum for use in FERRET by expanding the 45-group trial input spectrum to a 620-group structure using a spline interpolation procedure. The 620 point spectrum was then collapsed into the 53-group structure used in FERRET. The dosimeter sensor set reaction cross-sections obtained from the dosimetry file are also collapsed into the 53 energy group structure. The trial input spectrum, as expanded to 620 groups, is employed as a weighting function in the cross-section collapsing procedure.

FERRET employs a log-normal least squares algorithm and weights both the trial input values and measured reaction rate data in accordance with the assigned uncertainties and correlations and produces a best fit to the data.

INTVAL calculates the general parameters of neutron flux and uncertainties from the calculated and best estimate neutron spectra and group uncertainties. It also summarizes the measured, calculated, and best estimate reaction rates.

3. RESULTS AND DISCUSSIONS

3.1 Calculation Results

The three-dimensional multi-group neutron flux for each fuel cycle was calculated by using the synthesis technique described in section 2.1 at all reactor geometry. And then the fast neutron flux (E > 1 MeV) was obtained by integrating the multi-group flux above 1 MeV, and the associated fluence was also calculated by equation (5) using the full power operation time for each fuel cycle at all reactor geometry.

Figure 5 shows the fast (E > 1 MeV) neutron flux and fluence evaluated by the synthesis technique at the location of 5th capsule sensor set for Kori Unit 3. The 5th capsule is located at azimuthal angle of 20º relative to the core major axes as shown in Figure 1. In the case of pressure vessel, the maximum flux occurred at the azimuthal angle

of 0º and axial location between ±60cm from the core mid point, which is dependent on the core axial power shape of each fuel cycle.

Figure 6 shows the maximum fast (E > 1 MeV) neutron flux and fluence irradiated on the reactor pressure vessel inner surface (limiting region) for each fuel cycle. The value of cycle maximum fast neutron flux of the vessel inner surface is mainly affected by the relative powers of fuel assemblies close to this point, and the relative powers of these assemblies are highly dependent on the core loading pattern. Low leakage core loading pattern makes low neutron exposure on the pressure vessel.

Figure 7 shows the axial profile of the fluence (E > 1 MeV) distribution at the end of Cycle 15 along the core axial position at the azimuthal angle 0° on inner surface of pressure vessel. As shown in this figure the fast neutron fluence distribution is almost uniform within the range between ±100cm from the core center position. In this analysis the maximum fluence at the end of cycle 15 occurred at 37cm below from core center position.

3.2 Measurement Results

Dosimetry sensor set withdrawn from the 5th surveillance capsule of Kori Unit 3 were evaluated by the methodology described in section 2.3. Specific activity of each dosimetry sensor was determined using the ASTM counting procedures [8-14] and then the measured reaction rates were evaluated by FCALC [16] computer code. In this evaluation the monthly core power history taken from the site power history document were used (Figure 4).

Table 2 shows the measured specific activities and corresponding reaction rates for each dosimetry sensor evaluated using the dosimetry evaluation methodology described in section 2.3.

3.3 Comparisons of Calculations and Measurements

The average multi-group neutron spectrum during the whole irradiation periods (from Cycle 1 to Cycle 15) can be calculated by dividing the multi-group fluence at the end of Cycle 15 by the total irradiation time. This average neutron spectrum was used as a trial input spectrum of SAND/FERRET/INTVAL computer code sequence process described in section 2.4. In this process the measured reaction rates obtained in section 3.2 were also used to produce the best estimate neutron spectrum by the least square fit.

The calculated and the best estimated neutron spectrum are shown in Table 3. The calculated spectrum is the average neutron spectrum calculated by three-dimensional synthesis technique over the fifteen cycles at the location of dosimetry sensor set, on the other hand, the best estimate spectrum is the result obtained from the least square fit by SAND/FERRET/INTVAL computer code sequence using the measured reaction rates. The fast (E > 1 MeV) neutron flux can be easily obtained by integrating these spectra over the energy range above 1 MeV. The calculated flux

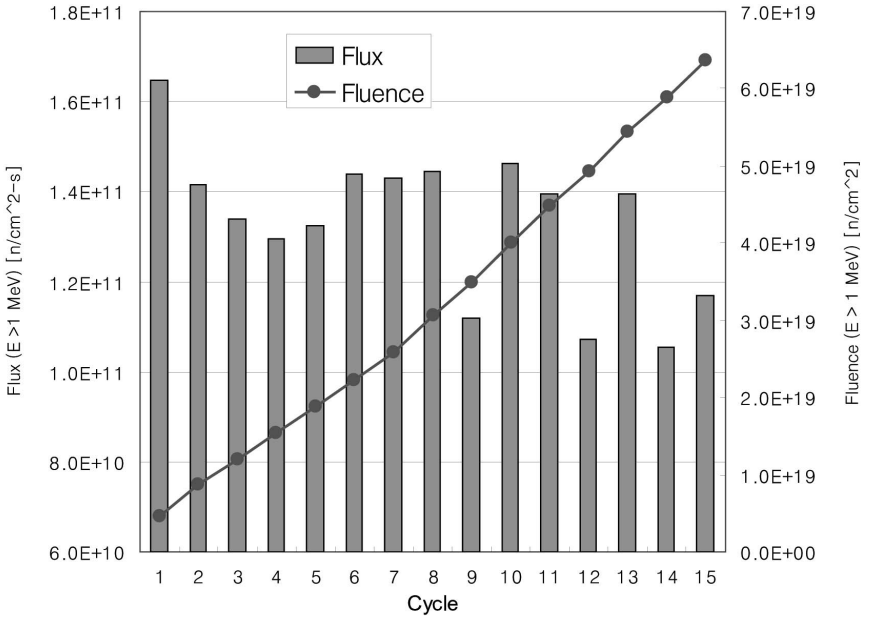

Fig. 5. Fast Neutron Flux and Fluence Evaluated by Synthesis Technique at the Location of 5th Capsule Dosimeter Set for Kori Unit 3

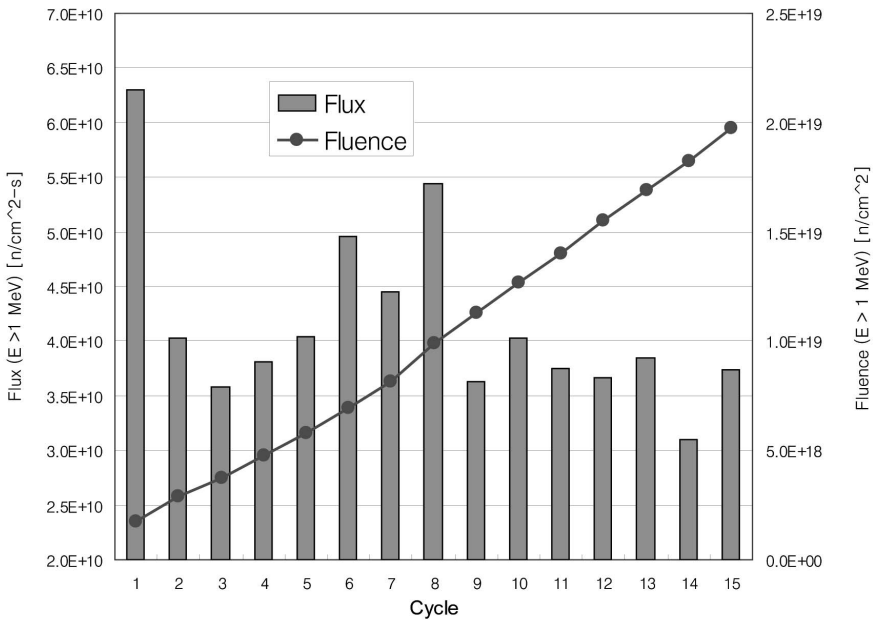

Fig. 6. Fast Neutron Flux and Fluence Evaluated by Synthesis Technique at the Location of Maximum Fluence Occurred for Kori Unit 3 Pressure Vessel Inner Surface

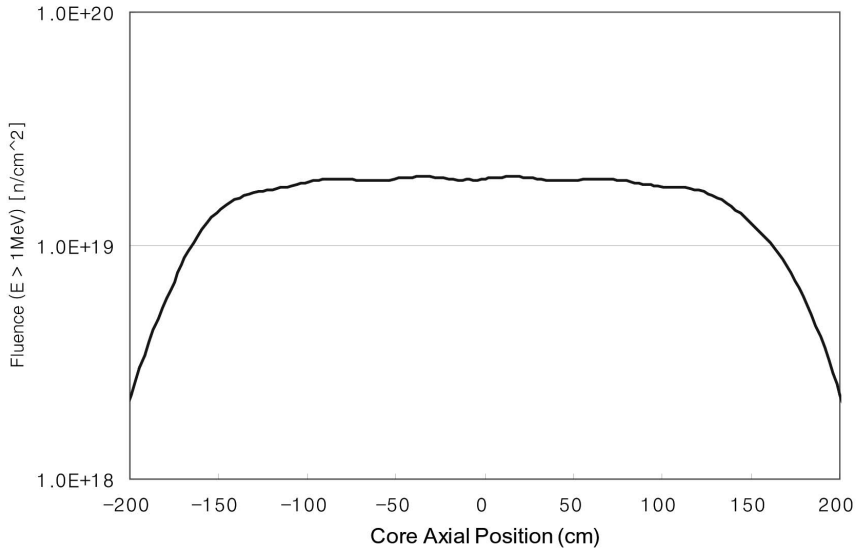

Fig. 7. Fast Neutron Fluence Distribution at the End of Cycle 15 Along the Core Axial Position at Azimuthal Angle 0º on Inner Surface of Pressure Vessel for Kori Unit 3

are 1.33E+11 n/cm^2-s and the best estimated fast neutron flux is 1.22E+11 n/cm^2-s with 6% uncertainty (1 σ level), and thus the ratio of best estimation to calculation is 0.92 which is called as bias factor. From the above result it can be said that the calculation model used in this paper makes an over estimation by 8% compared to the measurement in the location of dosimetry sensor set. The difference between the calculation and measurement is due to the uncertainties from the reactor dimension, coolant temperature, power distribution, as well as from other parameters. This bias factor can be applied to the synthesized three-dimensional neutron flux of all reactor geometry in order to obtain the

Table 2. Summary of Measured and Calculated Reaction Rates of Dosimetry Sensors Used in 5th Surveillance Capsule for Kori Unit 3

Reaction of Interest	Measured Specific Activity (dps/g)	Measured Reaction Rate per Atom	Calculated Reaction Rate per Atom	M/C Ratio
$^{63}Cu(n,\alpha)^{60}Co$	3.33E+05	6.74E-17	6.71E-17	1.00
$^{54}Fe(n,p)^{54}Mn$	3.76E+06	7.14E-15	7.62E-15	0.94
$^{58}Ni(n,p)^{58}Co$	5.98E+07	9.93E-15	1.07E-14	0.93
$^{238}U(n,f)^{137}Cs$	2.50E+06	3.77E-14	4.14E-14	0.91
$^{237}Np(n,f)^{137}Cs$	1.65E+07	3.63E-13	4.14E-13	0.88
$^{59}Co(n,\gamma)^{60}Co$	3.02E+07	2.61E-12	2.85E-12	0.92*
Average M/C Ratio for the fast neutron sensors				0.93

* Not fast neutron sensor, excluded from M/C averaging

Table 3. Summary of Trial and Best Estimated Flux and Uncertainties by groups from the SAND/FERRET/INTVAL Code Sequence

Gp	Energy (MeV)	Trial (n/cm^2-s)	BE (n/cm^2-s)	% Unc. 1 σ	Gp	Energy (MeV)	Trial (n/cm^2-s)	BE (n/cm^2-s)	% Unc. 1 σ
1	1.73E+01	8.21E+06	8.19E+06	13	28	9.12E-03	2.32E+10	2.24E+10	53
2	1.49E+01	1.77E+07	1.76E+07	12	29	5.53E-03	2.40E+10	2.32E+10	53
3	1.35E+01	6.56E+07	6.52E+07	11	30	3.36E-03	7.78E+09	7.52E+09	53
4	1.16E+01	1.82E+08	1.80E+08	10	31	2.84E-03	7.63E+09	7.38E+09	53
5	1.00E+01	4.26E+08	4.19E+08	9	32	2.40E-03	7.59E+09	7.32E+09	53
6	8.61E+00	7.59E+08	7.39E+08	7	33	2.04E-03	2.31E+10	2.22E+10	52
7	7.41E+00	1.88E+09	1.81E+09	7	34	1.23E-03	2.38E+10	2.27E+10	51
8	6.07E+00	2.94E+09	2.80E+09	6	35	7.49E-04	2.34E+10	2.22E+10	49
9	4.97E+00	6.13E+09	5.76E+09	6	36	4.54E-04	1.76E+10	1.66E+10	47
10	3.68E+00	7.25E+09	6.74E+09	6	37	2.75E-04	1.97E+10	1.85E+10	45
11	2.87E+00	1.43E+10	1.32E+10	7	38	1.67E-04	2.13E+10	1.95E+10	10
12	2.23E+00	1.96E+10	1.79E+10	7	39	1.01E-04	2.12E+10	1.99E+10	44
13	1.74E+00	2.74E+10	2.49E+10	8	40	6.14E-05	2.10E+10	1.98E+10	46
14	1.35E+00	3.17E+10	2.88E+10	9	41	3.73E-05	2.02E+10	1.92E+10	48
15	1.11E+00	5.96E+10	5.41E+10	10	42	2.26E-05	1.91E+10	1.83E+10	50
16	8.21E-01	6.43E+10	5.85E+10	11	43	1.37E-05	1.78E+10	1.72E+10	51
17	6.39E-01	7.46E+10	6.81E+10	12	44	8.32E-06	1.61E+10	1.57E+10	52
18	4.98E-01	4.84E+10	4.45E+10	13	45	5.04E-06	1.39E+10	1.36E+10	52
19	3.88E-01	7.76E+10	7.18E+10	14	46	3.06E-06	1.23E+10	1.21E+10	52
20	3.02E-01	7.53E+10	7.01E+10	15	47	1.86E-06	1.08E+10	1.06E+10	53
21	1.83E-01	8.13E+10	7.63E+10	15	48	1.13E-06	6.23E+09	6.17E+09	53
22	1.11E-01	4.56E+10	4.31E+10	16	49	6.83E-07	6.20E+09	7.43E+09	100
23	6.74E-02	4.45E+10	4.23E+10	16	50	4.14E-07	8.44E+09	1.20E+10	96
24	4.09E-02	2.17E+10	2.07E+10	17	51	2.51E-07	7.44E+09	1.27E+10	89
25	2.55E-02	2.72E+10	2.60E+10	17	52	1.52E-07	6.56E+09	1.29E+10	81
26	1.99E-02	1.08E+10	1.04E+10	17	53	9.24E-08	1.45E+10	4.32E+10	30
27	1.50E-02	2.09E+10	2.01E+10	17					

best estimate flux. Using this bias factor, the best estimated value for the maximum fast (E > 1 MeV) neutron fluence of the pressure vessel at the end of Cycle 15 was evaluated as 1.81E+19 n/cm^2, this value can be used in equation (3) to assess the state of embrittlement of the pressure vessel.

Another case for the validation of the calculation is to compare the reaction rates between calculation and measurement, which is shown in Table 2. The measured reaction rates (the third column of this table) are the dosimetry sensor reaction rates derived from the measured specific activities, on the other hand, the calculated reaction rates (the fourth column of this table) are those derived from the calculated neutron spectrum and dosimetry cross-section. The ratios (measurement/calculation) are also listed in this table and the results shows that the calculated values are in good agreement compared to the measurements for various neutron energy ranges. These results can be used in the assessment of the state of embrittlement of Kori Unit 3 pressure vessel.

REFERENCES

[1] Code of Federal Regulations Title 10 Part 50, "Domestic Licensing of Production and Utilization Facilities," Appendix G, "Fracture Toughness Requirement" and Appendix H, "Reactor Vessel Materials Surveillance Requirements," January 1992.

[2] Regulatory Guide 1.190, "Calculational and Dosimetry Methods for Determining Pressure Vessel Neutron Fluence," U. S. Nuclear Regulatory Commission, Office of Nuclear Regulatory Research, March 2001.

[3] L. R. Singer, "Korea Electric Power Corporation Korea Nuclear Unit No.7 Reactor Vessel Radiation Surveillance Program," WCAP-10777, Westinghouse, March 1985.

[4] RSICC Computer Code Collection CCC-650, "DOORS 3.1, One-, Two and Three-Dimensional Discrete Ordinates Neutron/Photon Transport Code System," August 1996.

[5] RSIC Data Library Collection DLC-185, "BUGLE-96, Coupled 47 Neutron, 20 Gamma-Ray Group Cross Section Library Derived from ENDF/B-VI for LWR Shielding and Pressure Vessel Dosimetry Applications," March 1996.

[6] Westinghouse Electric Company LLC, "SORCERY User Manual," December 2001.

[7] Regulatory Guide 1.99, Revision 2, "Radiation Embrittlement of Reactor Vessel Materials," U. S. Nuclear Regulatory Commission, May 1988.

[8] ASTM Designation E523-01, Standard Test Method for Measuring Fast-Neutron Reaction Rates by Radioactivation Of Copper, in 2002 Annual Book of ASTM Standards, Volume 12.02, ASTM, West Conshohocken, PA, 2002.

[9] ASTM Designation E263-00, Standard Test Method for Measuring Fast-Neutron Reaction Rates by Radioactivation of Iron, in 2002 Annual Book of ASTM Standards, Volume 12.02, ASTM, West Conshohocken, PA, 2002.

[10] ASTM Designation E264-92 (Reapproved 1996), Standard Test Method for Measuring Fast-Neutron Reaction Rates by Radioactivation of Nickel, in 2002 Annual Book of ASTM Standards, Volume 12.02, ASTM, West Conshohocken, PA, 2002.

[11] ASTM Designation E704-96, Standard Test Method for Measuring Reaction Rates by Radioactivation of Uranium-238, in 2002 Annual Book of ASTM Standards, Volume 12.02, ASTM, West Conshohocken, PA, 2002.

[12] ASTM Designation E705-96, Standard Test Method for Measuring Reaction Rates by Radioactivation of Neptunium-237, in 2002 Annual Book of ASTM Standards, Volume 12.02, ASTM, West Conshohocken, PA, 2002.

[13] ASTM Designation E481-97, Standard Test Method for Measuring Neutron Fluence Rate by Radioactivation of Cobalt and Silver, in 2002 Annual Book of ASTM Standards, Volume 12.02, ASTM, West Conshohocken, PA, 2002.

[14] ASTM Designation E1005-97, Standard Test Method for Application and Analysis of Radiometric Monitors for Reactor Vessel Surveillance, in 2002 Annual Book of ASTM Standards, Volume 12.02, ASTM, West Conshohocken, PA, 2002.

[15] Kori Unit 3 Final Safety Analysis Report, 1983.

[16] Westinghouse Electric Company LLC, "FCALC User Manual," November 1997.

[17] Westinghouse Electric Company LLC, "Kewaunee Reactor Pressure Vessel Fluence Evaluation," CN-REA-02-42, July 02, 2002.

[18] Westinghouse Electric Company LLC, "Benchmark Testing of the FERRET Code for Least Squares Evaluation of Light Water Reactor Dosimetry," WCAP-16083-NP Rev. 0, May 2004.

[19] Westinghouse Electric Company LLC, "SAND/FERRET/INTVAL User Manual," November 1997.

[20] RSIC Data Library Collection DLC-178, "SNLRML Recommended Dosimetry Cross-Section Compendium," July 1994.